arXiv:1207.3852v1 [cond-mat.supr-con] 17 Jul 2012

Electronic Nematicity in Pseudogap-like Phase diagram of $\mathrm{NaFe}_{1-x}\mathrm{Co}_x\mathrm{As}$

A. F. Wang,[1] J. J. Ying,[1] X. G. Luo,[1] Y. J. Yan,[1] D. Y. Liu,[2] Z. J. Xiang,[1] P. Cheng,[1] G. J. Ye,[1] L. J. Zou,[2] Z. Sun,[3] and X. H. Chen[1,] *
[1] *Hefei National Laboratory for Physical Science at Microscale and Department of Physics, University of Science and Technology of China, Hefei, Anhui 230026, People's Republic of China*
[2] *Key Laboratory of Materials Physics, Institute of Solid State Physics, Chinese Academy of Sciences, P. O. Box 1129, Hefei 230031, China*
[3] *National Synchrotron Radiation Laboratory, University of Science and Technology of China, Hefei, Anhui 230029*

Electronic nematicity, which breaks the C_4 rotational symmetry of underlying lattice, has been observed by various techniques in underdoped ferropnictides, accompanying the structural transition from tetragonal to orthorhombic. Recent magnetic torque measurements suggest that the electronic nematicity develops above the structural and superconducting transitions. However, there lacks evidence directly related to electronic excitations for the nematic transition. Symmetry breaking in electronic states can change low-lying electronic excitations and manifest itself in transport properties. Here we report electronic transport measurements on single crystals of $\mathrm{NaFe}_{1-x}\mathrm{Co}_x\mathrm{As}$ system. We found that the cotangent of Hall angle, $\cot\theta_{\mathrm{H}}$, follows T^3-dependence in all the superconducting samples. A deviation develops below a characteristic temperature T^* well above the structural and superconducting transitions, accompanied by a departure from power-law temperature dependence and the emergence of in-plane anisotropy in resistivity. These properties signify the emergence of electronic nematicity, which is found to exist in the whole superconducting regime. The doping dependence of T^* resembles the crossover line of pseudogap phase in cuprates. Our finding suggests that the electronic nematicity plays an important role for superconductivity.

The ferropnictide and cuprate high-temperature superconductors share some key similarities - an antiferromagentism in parent compounds, the quasi-two-dimensional nature of superconducting CuO_2 and $FeAs$ layers [1–5], and the emerging superconductivity realized by suppressing the antiferromagnetic ground states [6, 7]. A natural question is whether the two families have the same mechanism for superconductivity. In cuprate compounds, the nature of pseudogap phase is a key issue in understanding the high-temperature superconductivity. The evidence from resistivity [8], Nernst effect [9], inelastic neutron scattering [10–12] and scanning tunnelling spectroscopy [13, 14] indicated that the pseudogap phase is an electronic state that breaks rotational symmetry of underlying lattice with stripe or nematic order. Compared with the phase diagram of cuprates, the current interest in ferropnictides lies in the peculiar normal-state properties of these materials to detect whether there exists a pseudogap-like state.

In ferropnictides, the electronic nematicity has been detected by in-plane resistivity anisotropy [15], band structure measurements [16], scanning tunnelling spectroscopy [17] and inelastic neutron scattering [18]. In these studies, the structural distortions that break the crystal's C_4 rotational symmetry may apply external driving forces to induce the electronic nematicity. Very recently, magnetic torque measurements by Kasahara *et al.* revealed a nematic transition at high temperatures above the structural and superconducting transitions in $BaFe_2(As_{1-x}P_x)_2$, with a characteristic temperature similar to the pseudogap crossover in cuprate superconductors [19]. Without the potential external driving forces from the lattice, this transition can be considered to be induced by the electronic system only.

However, there lacks evidence directly related to the electronic properties of the high-temperature nematic transition reported by Kasahara *et al.*. For an evident phase transition, such as the superconducting, antiferromagnetic and structural transitions in ferropnictides, specific heat data show anomalies at corresponding temperatures (see the supplementary materials). In contrast, there is no such a feature in specific heat for the high-temperature nematic transition. It becomes nontrivial to locate the crossover line and determine the phase diagram. On the other hand, electronic transport measurements is a fine method to examine the nematic transition and can provide more clues on electronic behavior of the nematic state, because the symmetry breaking of nematicity can change the low-energy electronic excitations, though the precise microscopic origin and nature of the nematic state could be very different. In this report, we study the nematic state by the resistivity and Hall coefficient measurements on high-quality single crystals of $NaFe_{1-x}Co_xAs$. At high temperatures, the Hall angle, θ_{H}, reveals T^3-dependence for superconducting samples. Below a crossover temperature T^*, the resistivity and Hall angle deviate from power-law temperature depen-

---

*Corresponding author; Electronic address: chenxh@ustc.edu.cn

dence, and an in-plane anisotropic resistivity emerges, signifying the setting in of the nematic state. In the electronic phase diagram, T^* depicts a characteristic temperature similar to the pseudogap crossover in cuprate superconductors.

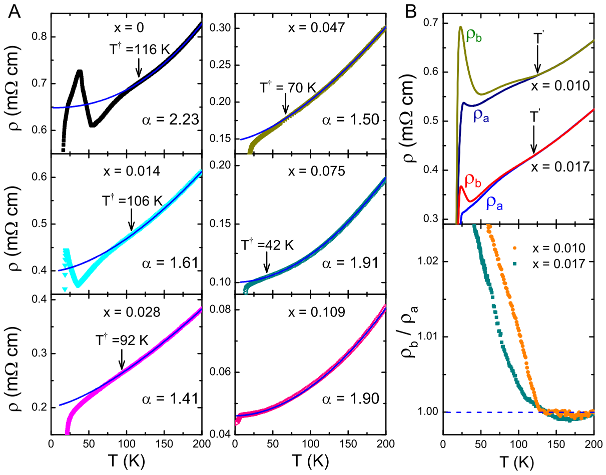

FIG. 1: (Color online) (**A**) Temperature dependence of in-plane resistivity, ρ_{xx}, for various crystals of $NaFe_{1-x}Co_xAs$. The solid lines are the fitting of in-plane resistivity *vs.* power-law temperature dependence, $\rho_{xx} = A + B \times T^{\alpha}$. A characteristic temperature, $T^{\dagger}$, is obtained, at which the resistivity deviates from the power-law behavior. The power-law exponent, α, decreases from 2.23 for the undoped crystal to 1.43 for the optimally doped sample, and then increases to 1.90 in the heavily overdoped non-superconducting crystal. To accurately determine the $T^{\dagger}$, we plot (ρ_{xx}-A)/T^{α} vs temperature in Fig.S4 (see supplementary information). In Fig.S4, one can easily see that ρ_{xx} starts to deviate from the power-law temperature dependence at $T^{\dagger}$. (**B**) *Upper panel*, in-plane resistivity of underdoped $NaFe_{1-x}Co_xAs$ crystals ($x = 0.010$ and 0.017) with the electric current flow along a and b directions, respectively; *Lower panel*, ρ_b/ρ_a for $x = 0.010$ and 0.017. The anisotropy starts at the T' marked by arrows, consistent with the temperature of $T^{\dagger}$.

We carefully measured the resistivity and Hall coefficient on single crystals of $NaFe_{1-x}Co_xAs$ system with $x = 0 - 0.109$ ranging from the parent compound to the heavily overdoped non-superconducting composition. Temperature dependence of resistivity is shown in the supplementary materials for all samples. The typical resistivity data are displayed in Fig.1A. For the parent compound and the underdoped crystals, there exists an upturn in resistivity below 50 K due to the structural and spin density wave (SDW) transitions [20]. An evident feature is that the resistivity curvature changes well above the T_{s} in parent compound and all underdoped samples. For the optimally doped and overdoped crystals, there seems no anomaly in the normal-state resistivity. In the high-temperature cuprate superconductors, the mapping of in-plane resistivity curvature is a useful way to determine electronic phase diagrams. In particular, the pseudogap crossover line can be conveniently obtained by this method [21]. Here, we made power law fitting on the resistivity data with formula $\rho_{xx} = A + B \times T^{\alpha}$ and show them in Fig.1A. One can see that the resistivity follows power-law dependence at high temperature and starts to deviate at a characteristic temperature, $T^{\dagger}$, for all the samples. The doping dependence of $T^{\dagger}$ will be shown in Fig. 4. For the heavily overdoped non-superconducting sample ($x = 0.109$), no deviation from the power-law dependence can be observed. Moreover, a consistent temperature scale can be obtained by the anisotropy of in-plane resistivity. The upper panel of Fig. 1B shows the temperature dependence of in-plane resistivity with the current flowing parallel to the orthorhombic a and b directions of detwinned crystals with $x = 0.010$ and 0.017, respectively. An evident anisotropy appears well above the T_s, being consistent with previous reports [15, 22]. In the lower panel of Fig.1B, the values of ρ_b/ρ_a start to deviate from 1 around 120 K, which are in excellent agreement with $T^{\dagger}$ (see Fig. 4). Here, we mark the temperature scale as T'.

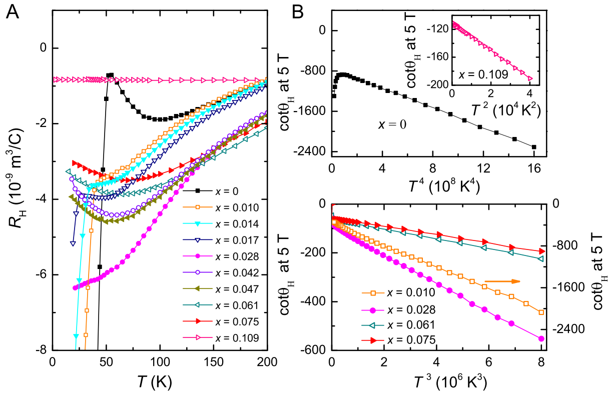

FIG. 2: (Color online) (**A**) Temperature dependence of Hall coefficient, R_H, for various single crystals of $NaFe_{1-x}Co_xAs$. (**B**) The cotangent of Hall angle, cotθ_{H}, *vs.* temperature power-law T^{α}, with $\alpha = 4$ for parent compound (upper panel), $\alpha = 3$ for all the superconducting crystals (lower panel), and $\alpha = 2$ for the heavily overdoped non-superconducting sample (inset of upper panel).

Figure 2A shows the temperature dependence of Hall coefficients, R_{H}, for various single crystals of $NaFe_{1-x}Co_xAs$. The Hall coefficients show a systematic evolution with increasing Co doping with a strong temperature dependence. The magnitude of Hall coefficients at room temperature increases upon Co doping, and then sharply decreases for the heavily overdoped non-superconducting sample with a value smaller than those of superconducting samples. It is worth noting that the Hall coefficient in the non-superconducting $x = 0.109$ compound is nearly independent of temperature, bearing a feature that is usually found in a conventional Fermi-liquid metal. This behavior suggests that

$NaFe_{1-x}Co_xAs$ becomes a traditional metallic material at very high doping levels. The abrupt increase below 50 K in magnitude of Hall coefficients for the underdoped samples is due to the structural transition. The complicated properties of temperature dependent Hall coefficients can be expressed in a simple fashion by looking at the cotangent of Hall angle: $\cot\theta_{\rm H} = \rho_{xx}/\rho_{xy}$ [23] as shown in Fig. 2B. It is interesting to notice that $\cot\theta_{\rm H}$ shows power-law temperature dependence for all the single crystals of $NaFe_{1-x}Co_xAs$: T^4 for the parent compound, approximately T^3 for all the superconducting crystals, and T^2 for the heavily-overdoped non-superconducting sample. T^α-dependent $\cot\theta_{\rm H}$ with α=2.5 ∼ 3.0 has been reported in $\rm BaFe_{2-x}Co_xAs_2$ single crystals[24]. In cuprates, $\cot\theta_{\rm H}$ behaves approximately as T^2 [23], regardless of materials and doping level, except that T^4-dependence is found in the electron-doped cuprates[25], which is interpreted by the multi-band effect with different contributions from various bands.

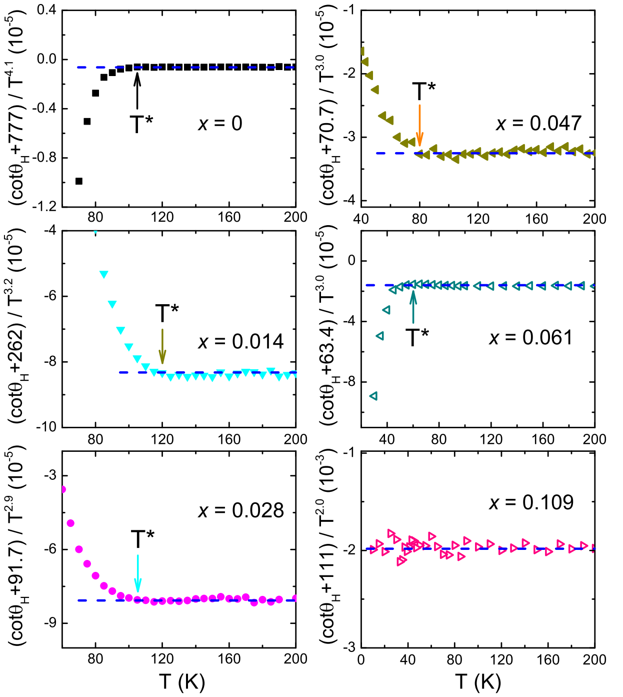

FIG. 3: (Color online) Plots of $(\cot\theta_{\rm H} - C)/T^\alpha$ *vs.* T for the single crystals of $NaFe_{1-x}Co_xAs$. The power-law temperature dependence of $\cot\theta_{\rm H}$ persists down to the characteristic temperature T^* (marked by arrows), and then a deviation starts.

A careful examination on Fig. 2B indicates slight curvatures in the plot, suggesting that the best power-laws in a wide temperature range deviate from an integer α. Fig. 3 shows plots of $(\cot\,\theta_{\rm H} - C)/T^\alpha$ *vs.* T for all the samples, in which the power-law temperature dependence is canceled out, so that one can easily see the temperature range in which the T^α behavior holds well. Here, C is the offset value and α is the best power. In Fig. 3, the power-law temperature dependent $\cot\theta_{\rm H}$ holds very well down to a characteristic temperature, T^*, for all the samples. Below T^*, $\cot\theta_{\rm H}$ departs from the power-law (T^α) behavior. This characteristic temperature decreases with increasing Co doping and goes to zero in the heavily overdoped non-superconducting sample.

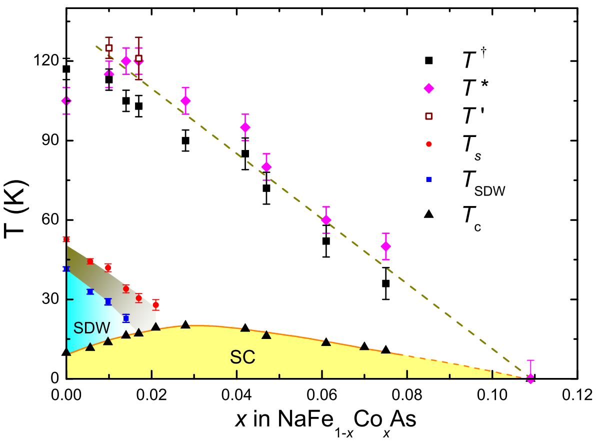

FIG. 4: (Color online) Phase diagram of $\rm NaFe_{1-x}Co_xAs$ system. The superconducting transition temperature, T_c, spin density wave (SDW) transition temperature, T_{SDW}, and structural transition temperature, T_s, were determined from resistivity, susceptibility and specific heat measurements by our group [20]. For the parent compound, the specific heat shows the structural and SDW transitions with no anomaly at T_c, suggesting a filamentary superconductivity. $T^\dagger$, T' and T^* were determined in Figs. 1A, 1B and Fig. 3, respectively. No anomaly is observed at $T^\dagger$ and T^* in specific heat measurements, suggesting these characteristic temperatures signify a nematic crossover, not a true phase transition.

Fig. 4 shows the phase diagram and we plot $T^\dagger$, T' and T^* determined in Fig. 1 and Fig. 3 as a function of doping. The three characteristic temperatures are highly consistent with each other, though they are obtained by different methods. Generally, both $T^\dagger$ and T^* decreases with increasing Co doping, and goes to zero at the doping level $x = 0.109$ where $T_{\rm c}$ goes to zero. The phase diagram in Fig. 4 is quite similar to the pseudogap phase diagram of the high-temperature cuprate superconductors. Indeed, the deviation of cot $\theta_{\rm H}$ from T^2 dependence has been used to characterize the onset of pseudogap in hole-doped cuprate superconductors [26], and the pseudogap crossover line can be conveniently determined by resistivity curvature mapping [21]. Here, these methods were used to determine the $T^\dagger$ and T^* and reveal the crossover line above the structural and superconducting transitions. Our data strongly suggests that a pseudogap-like crossover occurs at the T^* in ferropnictide superconductors.

A natural question is what happens below the T^*. Without the driving forces from structural or magnetic transitions, the T^* indicates a crossover with purely electronic origin. A highly plausible scenario is that the electronic nematic state sets in below the characteristic temperature. Indeed, a similar pseudogap-like crossover induced by electronic nematicity has been observed in $BaFe_2(As_{1-x}P_x)_2$ well above the structural and superconducting transitions[19]. The symmetry breaking of electronic states can affect the low-energy electronic excitations, which can manifest itself in the electronic transport measurements. Although there may exist many domains in a single crystal, the changes induced by the nematic symmetry breaking in individual domains can give rise to a global variation in electronic transport properties. The anisotropic behavior of in-plane resistivity shown in Fig. 1B is considered to be due to electronic nematicity. The temperature scale, T', is in excellent agreement with the $T^\dagger$ and T^* determined by resistivity and Hall angle (see Fig. 4). The consistency reinforces our point of view that the crossover temperature T^* or $T^\dagger$ in the phase diagram arises from the electronic nematicity.

Fig. 2B shows that the Hall angle exhibits approximate T^3-dependence for all the superconducting crystals, while the parent compound with filamentary superconductivity and the heavily overdoped non-superconducting crystal exhibit a different behavior. This finding suggests that the T^3-dependence of $\cot\theta_{\mathrm{H}}$ is tied to the superconducting region, though this behavior occurs right above the characteristic temperature of electronic nematicity. The electronic nematicity in multi-band ferropnictide compounds, driven either by the magnetic degeneracy of two SDW modes (π,0) and (0,π) through the Pomeranchuk instability [27–30], or by orbital order/fluctuations [31, 32], considerably affects the high-temperature transport properties of $NaFe_{1-x}Co_xAs$ through the nematic fluctuations. In Co-doped $NaFeAs$ compounds the conducting carriers consist of hole-type and electron-type. The former comes from the hole bands around the Γ point and the latter from the electron bands around the M point. The Hall angle determined by these two types of carriers reads:

$$cot\ \theta_H = \frac{\rho_h \rho_e(\rho_e + \rho_h)}{\rho_h^2 R_e + \rho_e^2 R_h} \tag{1}$$

with $\rho_{e,h}$ and $\mathrm{R}_{e,h}$ denoting the resistivities and Hall coefficients of the electron and hole carriers, respectively. Above T^*, the nematic order is destroyed by thermal excitations, and the nematic order parameter vanishes. However, the correlation scattering from nematic fluctuations gives rise to a non-Fermi liquid term in the resistivity of electron carriers, $\rho_e = a + b\times(T\text{-}T^*)$, though it has little effect on the resistivity of hole carriers. On the other hand, the electron-electron scattering dominates the resistivity of hole carriers, $\rho_h = AT^2/\epsilon_F^h$, due to the fact that the hole bandwidth is comparable with the thermal energy k_BT. The Hall coefficients of the hole and electron carriers are expected to be $\mathrm{R}\propto \alpha + \beta/T$. These components lead to a Hall angle with

$$cot\ \theta_H \approx C + \gamma T^3 \tag{2}$$

in the high temperature regime, where γ and C are two negative constants in the high-temperature regime, in accord with our data. Therefore, the consideration of nematic fluctuations, together with the contributions of the electron and hole bands to the resistivity, addresses the T^3-law of the Hall angle. A detailed theoretical analysis and the fitting to the experimental data are given in the supplementary materials. The fitting of Hall angle, Hall coefficient and resistivity by our model bear a self-consistent result. Given the facts that the nematic crossover covers the whole superconducting regime and that the T^3 of the Hall angle is tied to only superconducting compounds, our data suggest that electronic nematicity plays an important role for superconductivity.

Our electronic transport studies reveal the existence of electronic nematicity, which sets in at a crossover temperature well above structural and magnetic transitions. In the phase diagram of $NaFe_{1-x}Co_xAs$, the crossover line resembles the pseudogap phase diagram in cuprate superconductors. An interesting phenomenon is that the Hall angle reveals approximate T^3-dependence of $\cot\theta_{\mathrm{H}}$ in the whole superconducting regime, suggesting this behaivor is associated with bulk superconductivity in ferropnictides. The theoretical analysis based on the nematic fluctuation provides a reasonable explanation on T^3-dependence of $\cot\theta_{\mathrm{H}}$. These findings shed light on the mechanism of the high-temperature superconductivity in ferropnictides and potentially the superconductivity in cuprates as well.

X.H. Chen would like to thank Yayu Wang, Zheng-Yu Weng and J. P. Hu for stimulating discussion and suggestion. This work is supported by National Natural Science Foundation of China (Grant No. 11190021, 51021091), the National Basic Research Program of China (973 Program, Grant No. 2012CB922002 and No. 2011CB00101), and Chinese Academy of Sciences.

[1] Y. Kamihara *et al.*, J. Am. Chem. Soc. **130**, 3296(2008).
[2] X. H. Chen *et al.*, Nature **453**, 761(2008).
[3] C. De la Cruz et al., Nature **453**, 761(2008).
[4] M. Rotter *et al.*, Phys. Rev. Lett. **101**, 107006(2008).
[5] A. S. Sefat *et al.*, Phys. Rev. Lett. **101**, 117004(2008).
[6] P. A. Lee, N. Nagaosa and X. G. Wen, Rev. Mod. Phys. **78**, 17(2006).
[7] J. Paglione and R. L. Greene, Nature Phys. **6**, 645(2010).
[8] Y. Ando *et al.*, Phys. Rev. Lett. **88**. 137005(2002).
[9] R. Daou *et al.*, Nature **463**, 519(2010).
[10] C. Stock *et al.*, Phys. Rev. B **69**, 014502(2004).
[11] V. Hinkov *et al.*, Nature Phys. **3**, 780(2007).
[12] V. Hinkov *et al.*, Science **319**, 597(2008).
[13] Y. Kohsaka *et al.*, Science **315**, 1380(2007).
[14] Y. Kohsaka *et al.*, Nature **454**, 1072(2007).

[15] J. H. Chu *et al.*, Science **329**, 824(2010).
[16] M. Yi *et al.*, Proc. Natl. Acad. Sci. USA **108**, 6878(2011).
[17] T. M. Chuang *et al.*, Science **327**, 181(2010).
[18] J. Zhao *et al.*, Nature Phys. **5**, 555(2009).
[19] S. Kasahara *et al.*, Nature **486**, 382(2012).
[20] A. F. Wang *et al.*, Phys. Rev. B **85**, 224521(2012).
[21] Y. Ando *et al.*, Phys. Rev. Lett. **93**, 267001(2004).
[22] J. J. Ying *et al.*, Phys. Rev. Lett. **107**, 067001(2011).
[23] T. R. Chien, Z. Z. Wang and N. P. Ong, Phys. Rev. Lett. **67**, 2088(1991).
[24] E. Arushanov *et al.*, J. Supercond. Nov. Magn. **24**, 2285(2011).
[25] C. H. Wang *et al.*, Phys. Rev. B **72**, 132506(2005); Y. Dagan and R. L. Greene, Phys. Rev. B **76**, 024506(2007).
[26] Y. Abe, K. Segawa and Y. Ando, Phys. Rev. B **60**, 15055(R)(1999).
[27] S. A. Kivelson, E. Fradkin, and V. J. Emery, Nature **933**, 550 (1998); E. Fradkin *et al.*, Ann. Rev. Condens. Matt. Phys. **1**, 153 (2010).
[28] J. P. Hu, C. Setty, and S. Kivelson, Phys. Rev. B **85**, 100507(R) (2012).
[29] R. M. Fernandes, E. Abrahams, and J. Schmalian, Phys. Rev. Lett. **107**, 217002 (2011).
[30] H. Yamase and W. Metzner, Phys. Rev. Lett. **108**, 186405 (2012).
[31] W. C. Lv and P. Phillips, Phys. Rev. B **84**, 174512 (2011).
[32] D. Y. Liu *et al.*, Phys. Rev. B **84**, 064435 (2011).